Egyptian Journal of Radiology and Nuclear Medicine

RESEARCH

Open Access

Relationships of ^{18}F-FDG PET with tumor microenvironment immunotypes, especially PD-L1 and CD15 expression, and prognosis in oral squamous cell carcinoma

Mai Seki[1,2*], Takaaki Sano[1], Masaru Ogawa[2], Satoshi Yokoo[2] and Tetsunari Oyama[1]

Abstract

Background The relationship between 2-[18F]-fluoro-2-deoxy-D-glucose–positron emission tomography (FDG-PET) findings and programmed death ligand-1 (PD-L1) expression has been reported in several cancers. We investigated the correlations of FDG uptake with immune cell counts, including myeloid-derived suppressor cells (MDSCs), and PD-L1 expression in the tumor microenvironment. We examined 72 patients with oral squamous cell carcinoma (OSCC) with immunohistochemistry data for PD-L1, CD8, S100A8, CD15, and CD33. We used the maximum standardized uptake value (SUVmax) to reflect FDG uptake in each patient.

Results High SUVmax and high MDSC counts were associated with poor prognosis. Significantly higher SUVmax was found in patients with high PD-L1 expression and in those with a high $CD15^+$ cell density ($P=0.03$ and $P=0.02$, respectively). In multiple regression analysis, the tumor size had the greatest effect on SUVmax ($P<0.001$), followed by PD-L1 ($P=0.014$), and when the tumor size was excluded, CD15 ($P=0.02$) was included in the prediction equation. FDG uptake in some cold tumor subgroups, low PD-L1 expression, and a low $CD8^+$ cell density was linked to significantly lower SUVmax than the other variables. High SUVmax was clearly associated with high PD-L1 expression and/or a high $CD15^+$ cell density.

Conclusions FDG uptake was affected by PD-L1 expression and the density of $CD15^+$ cells in cancer tissue. FDG-PET may illuminate the tumor microenvironment immunotypes before biopsy or resection.

Keywords PD-L1, MDSC, FDG-PET, Oral, Squamous cell carcinoma

Background

Human cancers contain myeloid-derived suppressor cells (MDSCs), and the diverse populations of these cells trigger antitumor immunity [1]. In various cancer, it has been reported that MDSCs infiltrate peripheral blood and tumor tissues. In patients with oral squamous cell carcinoma (OSCC), increased MDSC counts within or around the tumor were obviously associated with poor prognosis [2]. In the microenvironment of oral cancer, programmed death ligand-1 (PD-L1) expression and the presence of immune cells have recently been reported [3, 4]. We also examined the number of immune cells, including PD-L1-positive cells and MDSCs in the tumor microenvironment in patients with OSCC using CD15 as a surrogate marker and found that MDSC counts were significantly lower in patients who showed tumor shrinkage [3].

*Correspondence:
Mai Seki
mai.s@gunma-u.ac.jp
[1] Department of Diagnostic Pathology, Gunma University Graduate School of Medicine, 3-39-22 Showa-machi, Maebashi, Gunma 371-8511, Japan
[2] Department of Oral and Maxillofacial Surgery, and Plastic Surgery, Gunma University Graduate School of Medicine, Maebashi, Gunma, Japan

According to PD-L1 status and the number of tumor-infiltrating lymphocytes (TILs), it is proposed to divide the tumor microenvironment into four groups: types I (PD-L1+ with TILs driving adaptive immune resistance), II (PD-L1 with no TILs, indicating immune ignorance), III (PD-L1+ with no TILs, indicating intrinsic induction), and IV (PD-L1 with TILs, indicating the function of other suppressors in promoting immunological tolerance) [5]

Tumors with a high density of infiltrating immune cells are called "hot" tumors and are thought to be more responsive to checkpoint inhibitor therapy than "cold" tumors with little or no local infiltration of immune cells [6]. MDSCs are among the factors that activate regulatory T cells (Tregs), suppress immune responses, and play an important role in the maintenance of the tumor's cold state in the tumor microenvironment [7].

2-[18F]-fluoro-2-deoxy-D-glucose–positron emission tomography (FDG-PET) is a non-invasive imaging modality for the differential diagnosis, characterization, and staging of malignant tumors [8, 9]. FDG-PET can be especially useful in the diagnosis of head and neck tumors, where tumor staging is an important prognostic factor that largely determines the therapeutic regimen [8, 9].

To date, many studies have reported PD-L1 expression and infiltrating immune cell counts in the tumor microenvironment [10–14]. Recently, the relationship between PD-L1 expression and FDG uptake was confirmed. Such reports in gastric [10], esophageal [15], breast [16], and lung cancers [17–20], suggested that high PD-L1 expression is correlated with high FDG uptake. Furthermore, a hot tumor immune status, which indicates high PD-L1 expression and the presence of $CD8^+$ lymphocytes, tends to portend a poor prognosis [15, 17]. Only one study investigating the relationship between FDG uptake and PD-L1 expression in oral cancer has been reported [21], and certain conclusions in OSCC have not yet been reached. Furthermore, no reports examined the effects of the tumor microenvironment immunotypes divided into the four aforementioned groups on the relationship between FDG uptake and MDSC counts in lesions including cancers of other organs.

In this study, we revealed the correlations of FDG uptake with PD-L1 and CD8 expression in OSCC. Furthermore, we investigated the correlation between FDG uptake and the counts of immune cells including MDSCs in the tumor microenvironment in patients with OSCC via immunohistochemistry using CD15, CD33, or S100A8 as the surrogate marker. We also identified the factor most strongly associated with FDG uptake and evaluated the relationship with prognosis.

Methods

We examined 72 patients with OSCC treated at our hospital between April 2018 and December 2019. Cases in which pathology specimens were not available, such as biopsies performed at other hospitals, and cases with a history of another oral cancer were excluded from the study because recurrence could not be ruled out. Patients in this study were followed-up for 2 years 6 months (median 18 months). Relapse cases consisted of local recurrences and lymph node or distant metastasis. There were 15 relapses and three relapse deaths. The clinicopathological details of the patients are presented in Table 1. We measured tumor size through clinical inspection at first medical examination with reference to imaging data such as those acquired using CT, MRI, and ultrasonography**.** All patients underwent 18F-FDG-PET for preoperative assessment. Seventy cases underwent FDG-PET after biopsy. Forty-two patients received preoperative S-1 chemotherapy, and the remaining 30 patients did not receive chemotherapy before surgery. Fundamentally, S-1 was orally administered before surgery at a dose of 80–120 mg/day according to the preoperative waiting period (mean, 11.1 days; median, 14 days; range, 1–28 days). The internal dose was dependent on the patient's body surface area. All patients finally underwent local tumor excision. Patient follow-up was performed through clinical observation, CT, MRI, and FDG-PET imaging. Diagnoses of local recurrent lesions were performed through biopsy or resected lymph nodes. Distant metastases were diagnosed according to a combination of imaging findings such as those acquired using CT, MRI, and FDG-PET. The study was approved by the Institutional Review Board for Clinical Research.

PET

Prior to the PET scan, all patients fasted for at least 6 h. The scan was performed using a PET/CT scanner with a 700-mm field of view (Discovery STE; GE Healthcare, Fairfield, CT, USA). After that, we simulated the capture of three-dimensional data 50 min after intravenously administering 5 MBq/kg 18F-FDG. We acquired four to 10 bed positions (3-min acquisition per bed position) according to the range of the imaging. Attenuation-corrected transverse images obtained with 18F-FDG were reconstructed with the ordered-subsets expectation maximization algorithm into 128×128 matrices with a slice thickness of 3.27 mm. All 18F-FDG images were interpreted by two experienced nuclear physicians. The physicians were unaware of the patient's clinical history and pathological data. Any discrepancies between the physicians were resolved by consensus. Functional images of the standardized uptake value (SUV) were produced using attenuation-corrected trans-axial

Table 1 Univariate and multivariate analysis of clinical and pathological variables for relapse

Clinicopathological factors	Total			Relapse (%)		Univariate analysis	Multivariate analysis		
				No	Yes	*P* value	*P* value	Odds ratio	95% CI
Total	72			57 (79)	15 (21)				
Clinical factors									
Age (mean: 69, range 23–94)									
< 70	30			25 (83)	5 (17)	0.56			
≥ 70	42			32 (76)	10 (24)				
Sex									
Male	32			25 (78)	7 (22)	0.85			
Female	40			32 (80)	8 (20)				
Primary site									
Tongue	41			31 (76)	10 (24)	0.56			
Other	31			26 (84)	5 (16)				
S-1 chemotherapy									
−	30			25 (83)	5 (17)	0.43			
+	42	No-responder	32	23 (55)	9 (45)	0.42			
		Responder	10	9 (90)	1 (10)				
cT									
T1/ T2	48			41 (85)	7 (15)	0.07			
T3/ T4	24			16 (67)	8 (33)				
FDG PET suv max									
Low (< 9.5)	44			39 (89)	5 (11)	***0.019***	0.10		
High (≥ 9.5)	28			18 (64)	10 (36)				
Pathological factor									
PDL-1									
Low (< 25%)	40			33 (83)	7 (17)	0.51			
High (≥ 25%)	32			24 (75)	8 (25)				
CD8									
Low	39			31 (79)	8 (21)	0.93			
High	33			26 (79)	7 (21)				
CD15									
Low	27			25 (93)	2 (7)	***0.017***	***0.028***	0.171	0.035–0.827
High	45			32 (71)	13 (29)				
S100A8									
Low	24			22 (92)	2 (8)	***0.025***	0.36		
High	48			35 (73)	13 (27)				
CD33									
Low	33			26 (79)	7 (21)	0.59			
High	39			31 (79)	8 (21)				

Statistically significant <0.05 is in bolditalic

images, the injected doses of 18F-FDG, the patients' body weight, and the cross-calibration factor between PET and the dose calibrator. We defined the SUV as follows: SUV = radioactive concentration in the region of interest (ROI) (MBq/g)/injected dose (MBq)/patient's body weight (g). The ROI was manually drawn over the primary tumor on SUV images. When the tumor was > 1 cm in diameter or if the shape of the tumor was irregular or multifocal, a ROI of approximately 1 cm in diameter was drawn over the area corresponding to the maximal tracer uptake. ROI analysis was performed by a nuclear physician with the aid of the corresponding CT scans. The maximal SUV in the ROI (SUVmax) was used as a representative uptake value for evaluating 18F-FDG uptake in each OSCC tumor. The average SUVmax in OSCC is 9.7 according to a previous report

from our institution [9]. The cutoff for low or high SUVmax was 9.5 in this study.

Variables of histopathology and immunohistochemistry

All histopathological and immunohistochemical variables were evaluated in biopsy specimens as some cases were affected by preoperative chemotherapy when evaluating resected specimens. According to the World Health Organization criteria, tumors < 2 cm in the greatest dimension were defined as T1, whereas those > 2 cm were given a grade of T2 or higher. The depth of invasion (mm) was measured from the surface of the tumor to the deepest point of an invasive tumor. Immunostaining was performed according to a routine protocol using mouse monoclonal antibodies against PD-L1 (28–8; 1:400 dilution; Abcam, Cambridge, UK), CD8 (C8/144B; 1:50 dilution; Nichirei, Tokyo, Japan), CD15 (Carb-3; 1:80 dilution; Dako), S100A8 (ab92331; 1:2000 dilution; Abcam), and CD33 (PWS44; 1:50 dilution; Leica). Antigen retrieval was performed by boiling samples for 30 min in 0.01 mol/L sodium citrate buffer (pH 6.0).

Immunohistochemistry evaluation

Immunohistochemistry for PD-L1, CD8, S100A8, CD15, and CD33 was performed using biopsy specimens from all patients. In this study, S100A8, CD33, and CD15 were used as immunohistochemical markers for MDSCs. PD-L1 expression was classified into 10% increments according to the positivity rate in the tumor cell membrane. In immunohistochemistry for CD8, S100A8, CD15, and CD33, the evaluation of positive cells was performed under light microscopy at the stroma at the invasive tumor front [3]. $CD8^+$, $S100A8^+$, $CD15^+$ and $CD33^+$ cells were counted in five fields at the invasive front at a magnification of × 400 (an area of approximately 228,906 μm^2), and the average number of cells was calculated for each sample. All immunohistochemical specimens were evaluated twice by one pathologist (M.S.S.) to exclude intra-observer variability.

Subgroups

Based on the result of receiver operator characteristic curves with variable cutoffs for a patient's prognosis with regards to PD-L1 expression and the densities of $CD8^+$, $CD15^+$, $S100A8^+$, and $CD33^+$ cells, cutoffs of 25% for PD-L1 expression, 111 for $CD8^+$ cell counts, 17 for

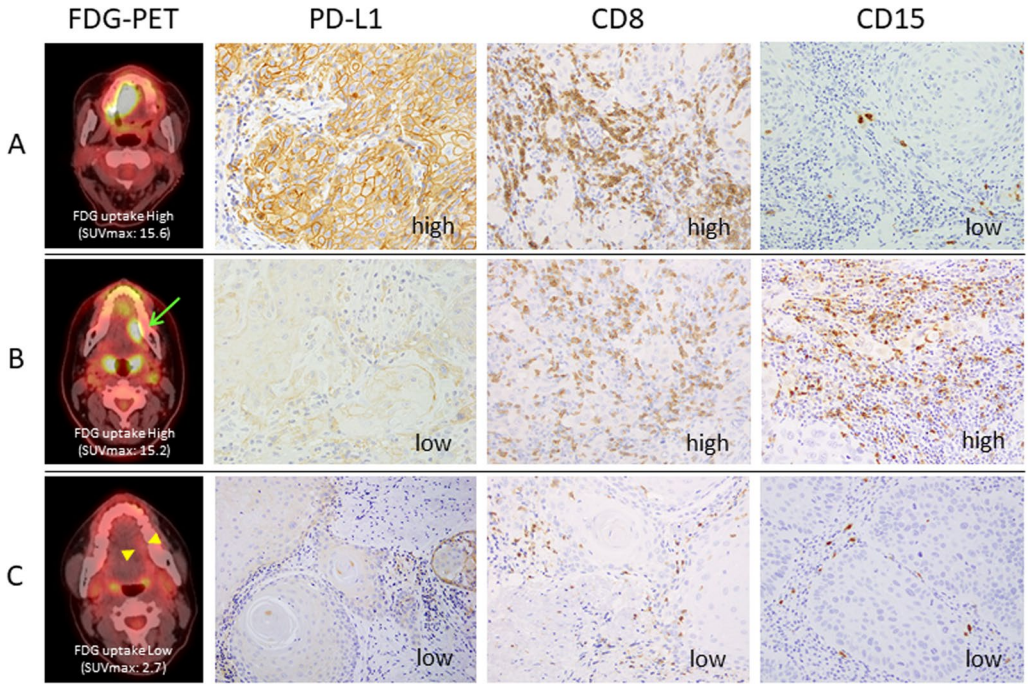

Fig. 1 Fluoro-D-glucose–positron emission tomography (FDG PET-CT) and immunohistochemical analysis of programmed death ligand-1 (PD-L1) expression, $CD8^+$ cells, and $CD15^+$ cells. Row **A** (a 76-year-old female patient with tongue cancer, cT4a), representing group I or group A (Fig. 3A), reveals high FDG uptake, high PD-L1 expression, high $CD8^+$ cell counts, and low $CD15^+$ cell counts. Row **B** (a 23-year-old female patient with tongue cancer, cT2), representing group IV or group D, presents high FDG uptake, low PD-L1 expression, and high $CD8^+$ and $CD15^+$ cell counts. Row **C** (a 32-year-old female patient with tongue cancer, cT1), belonging to group II or group C, reveals low FDG uptake, low PD-L1 expression, and low $CD8^+$ and $CD15^+$ cell counts

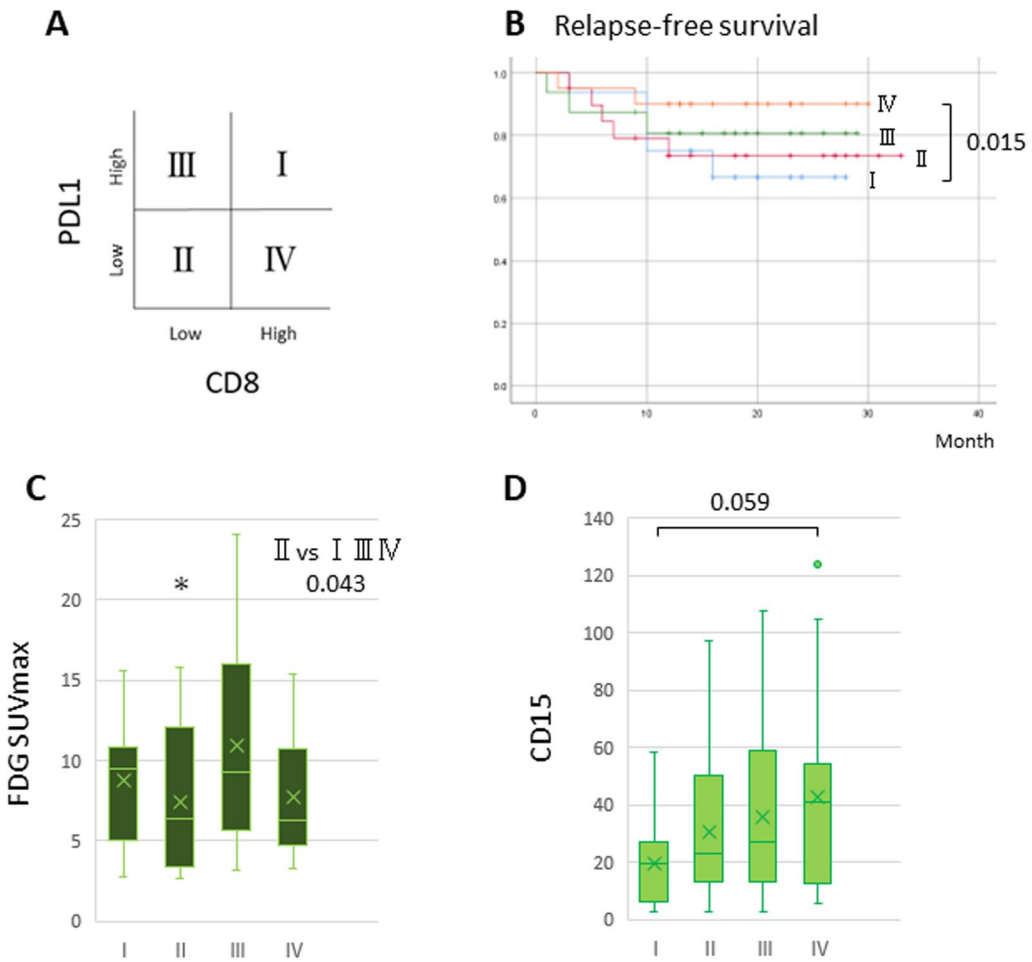

Fig. 2 **A** Patients were classified into four groups (I–IV) based on programmed death ligand-1 (PD-L1) expression in tumor cells and $CD8^+$ cell counts at the tumor invasive front. **B** Kaplan–Meier plots of relapse-free survival in the subgroups. The differences in survival between groups I (high PD-L1 expression and high density of $CD8^+$ cells) and IV (low PD-L1 expression and high density of $CD8^+$ cells) were statistically significant ($P = 0.015$). **C** Box-and-whisker diagrams present fluoro-D-glucose (FDG) uptake in the four subgroups. Group II (low PD-L1 expression and low density of $CD8^+$ cells) had significantly lower FDG uptake (indicated by the maximum standardized uptake value (SUVmax)] than the other groups ($P = 0.043$). **D** The density of $CD15^+$ cells at the tumor invasive front was not significantly different among the four groups, but comparing groups I and IV, both of which had high $CD8^+$ cell counts despite having high and low PD-L1 expression, respectively, group IV tended to have a higher density of $CD15^+$ cells than group I (**D**)

$CD15^+$ cell counts, 51 for $S100A8^+$ cell counts, and 10 for $CD33^+$ cell counts were employed (Fig. 1). Tumors were categorized into four groups based on PD-L1 expression in tumor cells and $CD8^+$ cell counts at the tumor invasive front as presented in Fig. 2A [5]. Groups I (high PD-L1 expression and high $CD8^+$ cell density) and IV (low PD-L1 expression and high $CD8^+$ cell density) represented hot tumors, and Groups II (low PD-L1 expression and low $CD8^+$ cell density) and III (high PD-L1 expression and low $CD8^+$ cell density) represented cold tumors [5]. Tumors were additionally classified into four groups based on PD-L1 expression in tumor cells and $CD15^+$ cell counts at the tumor invasive front (A–D) as presented in Fig. 3A, namely Groups A (high PD-L1 expression and low $CD15^+$ cell density), B (high PD-L1 expression and high $CD15^+$ cell density), C (low PD-L1 expression and low $CD15^+$ cell density), and D (low PD-L1 expression and high $CD15^+$ cell density).

Statistical analysis

The χ^2 test was used to analyze the clinicopathological variables according to the event. In univariate and multivariate analyses, $P < 0.05$ denoted statistical significance. The Student t test was used to compare SUVmax in the high and low groups and to compare two of each of the four subgroups (I–IV, A–D). Multiple regression was

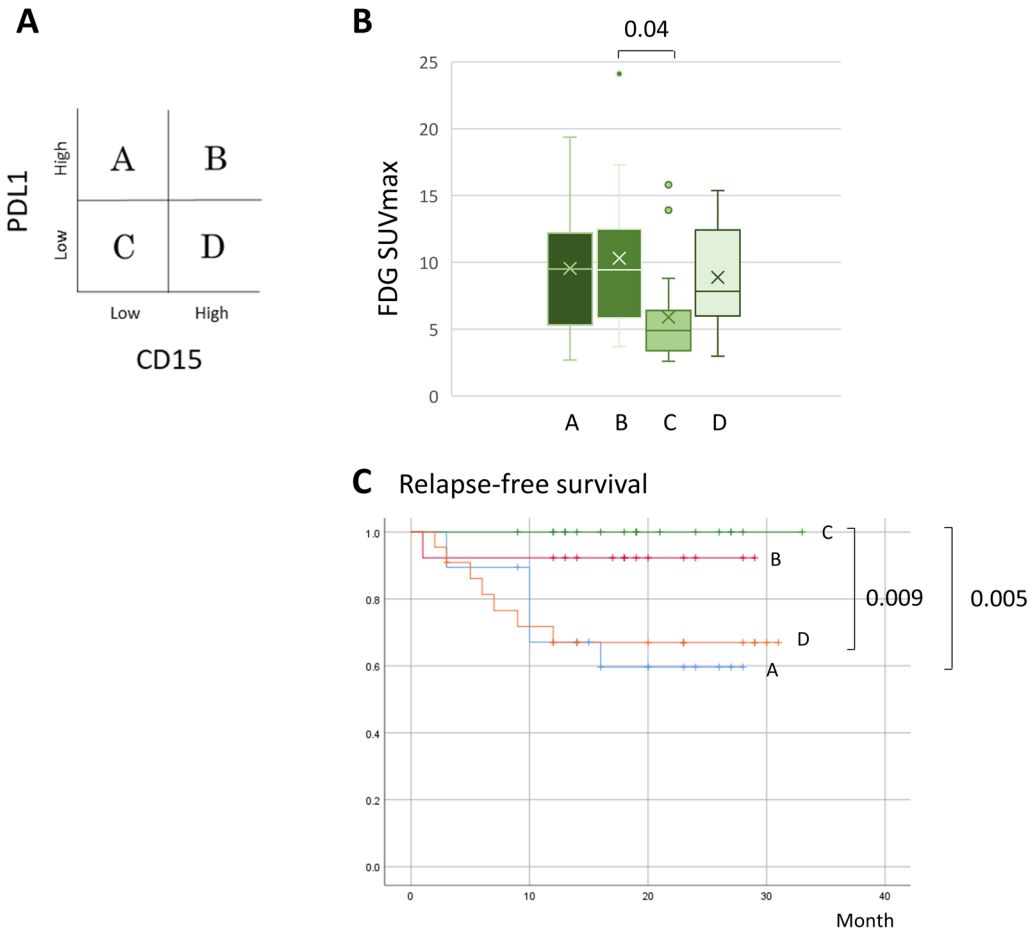

Fig. 3 **A** Patients were classified into four groups (A–D) based on programmed death ligand-1 (PD-L1) expression in tumor cells and $CD15^+$ cell counts at the tumor invasive front. **B** Box-and-whisker diagrams present fluoro-D-glucose (FDG) uptake in the four subgroups. Group C (low PD-L1 expression and low density of $CD15^+$ cells) had significantly lower FDG uptake (indicated by the maximum standardized uptake value [SUVmax]) than group B ($P=0.04$). **C** Kaplan–Meier plots of relapse-free survival in the subgroups. Group C had significantly better survival than groups A and D ($P=0.005$ and $P=0.009$, respectively) (high PD-L1 expression and high density of $CD15^+$ cells)

used to analyze the relationships between SUVmax and several independent variables. Relapse-free survival by group (I–IV, A–D) was determined using the Kaplan–Meier method and log-rank test. All statistical analyses were performed using IBM SPSS version 21 software (IBM Corp., Armonk, NY, USA).

Results

Clinicopathological results and prognosis

In the clinicopathological examination of patients with and without relapse, the numbers of $S100A8^+$ and $CD15^+$ cells at the invasive front and SUVmax were significantly associated with the risk of relapse in univariate analysis ($P=0.019$, Table 1). Specifically, patients with high $CD15^+$ expression, high $S100A8^+$ cell counts, and high SUVmax (≥ 9) had a significantly higher relapse rate. Multivariate analysis revealed that only $CD15^+$ cell counts were associated with the risk of relapse. In Kaplan–Meier plots of relapse-free survival (Additional file 1: Figure S1), high SUVmax and high MDSC cell counts ($CD15^+$ and $S100A8^+$) were associated with poor prognosis. High SUVmax was also linked to poor overall survival. The counts of $S100A8^+$ and $CD15^+$ cells were not associated with overall survival.

Relationship between FDG-PET and clinicopathological data

The relations between clinical variables and SUVmax values of FDG-PET are shown in Table 2, and these SUVmax values were significantly associated with cT and cStage. FDG uptake tended to be higher in the high S100A8, and CD33 expression groups, whereas $CD8^+$ cell counts tended to be lower in the high expression groups. Significantly higher SUVmax values were found in patients with higher PD-L1 expression and in those with higher $CD15^+$

Table 2 Univariate analysis of clinical variables for SUVmax of FDG-PET

Clinical factors	Total	FDG-PET(SUVmax)				Univariate analysis
		Low < 9.5	(%)	High ≥ 9.5	(%)	*P* value
Total	72	44	(61)	28	(39)	
FDG (SUVmax) mean		5.52		13.37		
Age						
< 70	30	20	(67)	10	(33)	0.47
≥ 70	42	24	(57)	18	(43)	
Sex						
Male	32	20	(63)	12	(37)	1.00
Female	40	24	(60)	16	(40)	
Primary site						
Tongue	41	26	(63)	15	(37)	0.81
Other	31	18	(58)	13	(42)	
cT						
T1	16	12	(75)	4	(25)	***< 0.001***
T2	32	26	(81)	6	(19)	
T3	10	4	(40)	6	(60)	
T4	14	2	(14)	12	(86)	
cStage						
I/II	44	35	(80)	9	(20)	***< 0.001***
III/IV	28	9	(32)	19	(68)	

Statistically significant <0.05 is in bolditalic

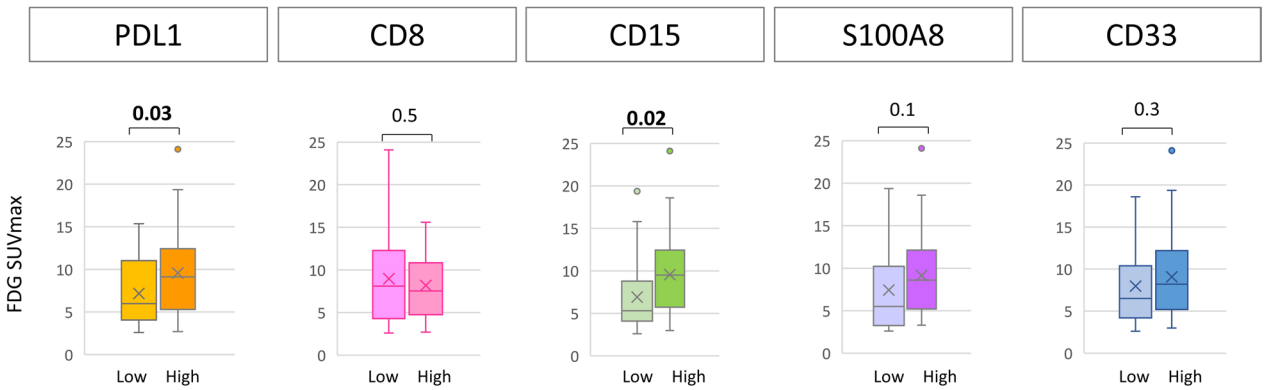

Fig. 4 Box-and-whisker diagrams show the distribution of the maximum standardized uptake value (SUVmax) in the high and low groups of programmed death ligand-1 (PD-L1) expression and $CD8^+$, $CD15^+$, $S100A8^+$ and $CD33^+$ cell counts. Significantly higher SUVmax, denoting higher fluoro-D-glucose uptake, was found in patients with PD-L1 expression group and in those with high $CD15^+$ cell counts ($P=0.03$ and $P=0.02$, respectively). There was no significant difference in SUVmax with respect to the number of $CD8^+$, $S100A8^+$, or $CD33^+$ cells

cell counts ($P=0.03$ and $P=0.02$, respectively) (Fig. 4). In correlation analysis, SUVmax was significantly associated with tumor size, $CD15^+$ and $S100A8^+$ cell counts, and PD-L1 expression. There was no significant correlation of SUVmax with $CD33^+$ or $CD8^+$ cell counts (Additional file 3: Table S1 and Additional file 2: Figure S2). In multiple regression analysis including all variables, tumor size had the strongest effect on SUVmax, followed by PD-L1, and when the tumor size was excluded, CD15 was included in the prediction equation (Table 3).

Relationships between PD-L1, CD8, and FDG-PET

In Kaplan–Meier plots of relapse-free survival in subgroups fractionated on the basis of PD-L1 and CD8 (Fig. 2A), the differences in survival between groups I and IV were statistically significant ($P=0.015$, Fig. 2B). Group I (high PD-L1 expression and high $CD8^+$ cell

Table 3 Results of multiple regression analysis for FDG PET

Model	Unstandardized coefficients (B)	Standardized coefficients	Significance (*p*)	95%CI
1. All variables				
(Constant)	2.842		0.031	0.274–5.410
Tumor size	0.158	0.400	< 0.001	0.076–0.241
PD-L1	0.051	0.263	0.014	0.010–0.091
2. Model excluding tumor size				
(Constant)	5.190		< 0.001	3.090–7.289
PD-L1	0.069	0.359	0.002	0.026–0.112
CD15	0.045	0.265	0.02	0.007–0.082

density, Fig. 1A) was linked to poor prognosis, whereas Group IV (low PD-L1 expression and high $CD8^+$ cell density, Fig. 1B) was linked to better prognosis. In box-and-whisker diagrams, there was no significant difference when two among the I–IV groups were compared, although Group II (low PD-L1 expression and low $CD8^+$ cell density, Fig. 1C), which was a cold tumor group, had significantly lower FDG uptake than the other groups (I + III + IV) ($P = 0.043$, Fig. 2C). Group IV tended to have higher $CD15^+$ cell counts than Group I, although statistical significance was not achieved ($P = 0.059$, Fig. 2D). The results shown in Fig. 2 indicate that FDG accumulation correlated with PD-L1 expression but not with that of CD8.

Relationships between PD-L1, CD15, and FDG-PET

In subgroups fractionated on the basis of PD-L1 and CD15 (Fig. 3A), high PD-L1 expression or a high $CD15^+$ cell density tended to be associated with high SUVmax and poor prognosis (Fig. 3B, 3C). In particular, Group C (low PD-L1 expression and low $CD15^+$ cell density, Fig. 1C) had significantly lower SUVmax than group B ($P = 0.04$, Fig. 3B). Group C had significantly better prognosis than groups A and D ($P = 0.005$ and $P = 0.009$, respectively) (high PD-L1 expression and high $CD15^+$ cell density, Fig. 1A, 1B).

Discussion

In recent years, the number of reports related to MDSCs and the cancer microenvironment has increased, including reports in head and neck [22] and oral cancers [2, 23, 24]. In addition, some reports used CD15 [3, 25], CD33 [26], and S100A8 [27] as surrogate markers for MDSCs in immunohistochemistry. In our previous study in OSCC [3], the degree of $CD15^+$ cell infiltration in the biopsy specimen was a good marker of recurrence and prognosis. Using the degree of $CD15^+$ cell infiltration around cancer cells, which indicates MDSC infiltration, we found that patients with a high $CD15^+$ cell density had a significantly higher recurrence rate [3]. The result represents evidence of immunosuppression in the cancer microenvironment by MDSCs.

We investigated the correlation betwen FDG uptake and PD-L1 expression and immune cell counts, including MDSCs. CD15, CD33, and S100A8 were used as surrogate markers in immunohistochemistry for MDSCs. CD15 was used as a marker of granulocytic MDSCs (G-MDSCs) in this study, although some neutrophils were also detected [25]. S100A8 is an inflammatory mediator released by neutrophils and monocytes, and it was used as surrogate marker of MDSCs including both G-MDSCs and monocytic MDSCs (M-MDSCs) [28]. In this study, the numbers of $CD15^+$ and $S100A8^+$ cells in the same samples were correlated, and more cells were positive for S100A8 than for CD15. Given the results that patients with a high $CD15^+$ or $S100A8^+$ cell density had poor prognoses, CD15 and S100A8 were considered useful markers for evaluating MDSCs in OSCC. In addition to PD-L1, the number of $CD15^+$ cells in cancer tissue was well correlated with SUVmax. Concerning prognosis, CD15, S100A8, and FDG uptake were significantly related to high recurrence rates, but only CD15 was significantly associated with recurrence in multivariate analysis.

Cancer cells use glucose as an energy source, and tumors with high proliferative potential are more likely to accumulate FDG [29]. SUV, a semi-quantitative indicator of FDG accumulation, reflects the malignancy of cancer cells, such as their survival, proliferation, apoptosis, p53 overexpression, and hypoxia [30]. SUV is reported to be a predictive factor for prognosis and therapeutic response in primary head and neck cancers [31–33]. In multiple regression analysis in this study, tumor size was most strongly related to SUVmax, followed by PD-L1. Excluding tumor size, it was revealed that CD15 was the next most relevant factor. In oral cancer, it has been reported that SUVmax is correlated with tumor size [34]. Studies investigating

the relationship between FDG uptake and PD-L1 expression in lung [17–20], gastric [10], esophageal [15], breast [16], and oral cancers have been recently reported [21]. In lung cancer, high SUVmax on FDG-PET was correlated with high PD-L1 expression [17–20]. Kuriyama et al. [15]. reported that high FDG uptake in esophageal squamous cell carcinoma was significantly associated with cancer aggressiveness, high PD-L1 expression and high $CD8^+$ cell counts, denoting the so-called hot tumor immune status. In breast cancer [16], patients with high FDG uptake also displayed high PD-L1 expression and high $CD8^+$ cell infiltration. These findings of a positive correlation between PD-L1 and FDG uptake aligned with our results in OSCC, although no correlation between FDG uptake and CD8 expression was found in OSCC. It is unclear why increased PD-L1 expression leads to increased FDG uptake. Intrinsically, PD-L1–expressing tumors tend to be high-grade tumors, which may result in increased FDG uptake. The uptake of FDG by tumor cells is closely related to glucose metabolism and hypoxia, and the expression of glucose transporter 1 (GLUT1), which is responsible for glucose metabolism, and HIF-1α, which responds to hypoxia, have been found to play important roles in FDG accumulation [35]. In patients with lung or kidney cancer, PD-L1 expression has been reported to be associated with GLUT1 and HIF-1α expression [36, 37]. Regarding the mechanism of FDG uptake, HIF-1α has been found to be an essential factor associated with the upregulation of GLUT1. Recent studies indicated that increased HIF-1α expression is associated with increased PD-L1 expression [38]. It has also been reported that HIF-1α binds directly to the hypoxia response element in the proximal promoter of PD-L1 and regulates its expression under hypoxia [39]. These results suggest that PD-L1 may be an alternative target of HIF-1α. Interestingly, HIF-1α has also been revealed to promote the accumulation of MDSCs, which is consistent with our findings [40]. The relationship between PD-L1 expression and FDG uptake needs to be further investigated.

In oral cancer, Togo et al. [21]. reported that cold tumors tend to exhibit high FDG uptake, contradicting our findings. In addition to differences of the evaluators, our study also included more recent cases and a slightly higher number of cases than their report. It was possible that our specimens were better preserved and that the immunohistochemistry result was more accurate because the cases were recent. Our results in this study were in good agreement with those in cancers in other organs.

No previous report examined the relationship between MDSCs in cancer tissue (including cancers of other organs) and FDG uptake. MDSCs are myeloid cells or neutrophils like cells and which means histologically high inflammatory cells infiltration in the tumor. It is speculated that the FDG uptake of the lesion in inflammatory states may be higher than the activity or proliferative potential of the tumor cells themselves. It has been reported that intra-abdominal lymph nodes that heavily infiltrated with MDSCs using S100A8/A9 as an indicator can be mistakenly detected as metastatic lymph nodes of cancer by FDG-PET [41]. In other words, tissues infiltrated by a large number of MDSCs may have higher FDG uptake. Considering that S-1, which suppresses MDSCs, had a strong antitumor effect in our previous study of OSCC, the impact of MDSCs on the tumor microenvironment in OSCC may be higher than observed in other cancers.

In subgroups fractionated on the basis of PD-L1 and CD8, Group II (low PD-L1 expression and low $CD8^+$ cell density), representing cold tumors, had significantly lower SUVmax. Group I (high PD-L1 expression and high $CD8^+$ cell density), representing hot tumors, had the worst poor prognosis, and this result is in good agreement with many previous studies in oral cancer, namely that PD-L1–overexpressing tumors have a poor prognosis and that PD-L1 expression is correlated with high $CD8^+$ cell infiltration [42]. In Group IV (low PD-L1 expression and high $CD8^+$ cell density), representing hot tumors, the reason for the low PD-L1 expression despite the high $CD8^+$ cell density was considered immunosuppression by cells such as MDSCs. In support of this hypothesis, Group IV tended to have higher $CD15^+$ cell counts in this study (Fig. 3D). Group IV had a significantly better prognosis than Group I in this study; however, this may be attributable to the active use of S-1, which has an inhibitory effect on MDSCs, preoperatively at our institution. We have created new subgroups fractionated on the basis of PD-L1 and CD15, the two factors in the immune microenvironment that affect FDG uptake. Patients with higher SUVmax values clearly displayed higher PD-L1 expression and/or $CD15^+$ cell counts. This suggests that clinically measured FDG-PET SUVmax values in OSCC may reflect the PD-L1 levels of tumor cells and the density of MDSCs in the tumor microenvironment, in addition to the biological growth potential of the tumor. In other words, OSCC with high FDG uptake may be considered high PD-L1 and/or high density MDSCs and may be an indication for anti-PD-L1 or anti-MDSC therapies even before biopsy or resection.

Limitations

Although the number of cases in this study is considered adequate, more than half of the patients were treated with preoperative chemotherapy, and histopathologic evaluation was performed on biopsy specimens. Future

evaluations of resected specimens that include a larger area or deeper tumors are desirable.

Conclusions

In OSCC, FDG uptake was affected by tumor size, tumor PD-L1 expression, and the density of $CD15^+$ cells in cancer tissue. Patients with high FDG uptake may be good candidates for PD-L1 blockade immunotherapy or MDSC-suppressing therapies such as S-1, and it may be possible to assess their suitability by FDG-PET before biopsy or resection.

Abbreviations

OSCC	Oral squamous cell carcinoma
FDG-PET	Fluoro-D-glucose–positron emission tomography
MDSCs	Myeloid derived suppressor cells

Supplementary Information

The online version contains supplementary material available at https://doi.org/10.1186/s43055-023-01025-w.

Additional file 1. Figure S1. Kaplan–Meier plots of relapse-free survival and overall survival. Patients with high fluoro-D-glucoseuptakeand high counts of myeloid-derived suppressor cellshad significantly worse relapse-free survival. High FDG uptake was also associated with significantly worse overall survival.

Additional file 2. Figure S2. Scatter plots presenting the correlation between CD15 and S100A8 and between FDG uptakeand CD15, programmed death ligand-1, S100A8, and tumor size.

Additional file 3. Table S1. Correlation between FDG-PET and pathological data.

Acknowledgements

We thank Futoshi Hara and Kumiko Suto for technical assistance with immunohistochemistry.

Author contributions

MS and TS reviewed the slides and wrote the paper. MO and SY provided the clinical information. TO provided expert pathological advice. All authors read and approved the final manuscript.

Funding

No funding was obtained for this study.

Availability of data and materials

The data are not publicly available due to privacy or ethical restrictions.

Declarations

Ethics approval and consent to participate

The study was approved by the Institutional Review Board for Clinical Research of Gunma University Hospital and conforms to the Declaration of Helsinki.

Consent for publication

Informed consent was obtained from all individual participants included in the study.

Competing interests

The authors declare that they have no competing interests.

Received: 2 March 2023 Accepted: 20 April 2023
Published online: 28 April 2023

References

1. Poschke I, Kiessling R (2012) On the armament and appearances of human myeloid-derived suppressor cells. Clin Immunol 144:250–268
2. Pang X, Fan HY, Tang YL et al (2020) Myeloid derived suppressor cells contribute to the malignant progression of oral squamous cell carcinoma. PLoS ONE 24:e0229089
3. Seki-Soda M, Sano T, Ogawa M et al (2021) $CD15^+$ tumor infiltrating granulocytic cells can predict recurrence and their depletion is accompanied by good responses to S-1 with oral cancer. Head Neck 43:2457–2467
4. Takahashi H, Sakakura K, Arisaka Y et al (2019) Clinical and biological significance of PD-L1 expression within the tumor microenvironment of oral squamous cell carcinoma. Anticancer Res 39:3039–3046
5. Teng MW, Ngiow SF, Ribas A et al (2015) Classifying cancers based on T-cell infiltration and PD-L1. Cancer Res 75:2139–2145
6. Gujar S, Pol JG, Kroemer G (2018) Heating it up: oncolytic viruses make tumors 'hot' and suitable for checkpoint blockade immunotherapies. Oncoimmunology. 7:e1442169
7. Zhu J, Petit PF, Van den Eynde BJ (2019) Apoptosis of tumor-infiltrating T lymphocytes: a new immune checkpoint mechanism. Cancer Immunol Immunother 68:835–847
8. Nakasone Y, Inoue T, Oriuchi N et al (2001) The role of whole-body FDG-PET in preoperative assessment of tumor staging in oral cancers. Ann Nucl Med 15:505–512
9. Miyashita G, Higuchi T, Oriuchi N et al (2010) ^{18}F-FAMT uptake correlates with tumor proliferative activity in oral squamous cell carcinoma: comparative study with ^{18}F-FDG PET and immunohistochemistry. Ann Nucl Med 24:579–584
10. Chen R., Chen Y., Huang G. et al (2919) Relationship between PD-L1 expression and (18)F-FDG uptake in gastric cancer. Aging Albany NY. 11: 12270-12277.
11. Svensson MC, Borg D, Zhang C et al (2019) Expression of PD-L1 and PD-1 in chemoradiotherapy-naïve esophageal and gastric adenocarcinoma: relationship with mismatch repair status and survival. Front Oncol 13:136
12. Marshall HT, Djamgoz MBA (2018) Immuno oncology: emerging targets and combination therapies. Front Oncol 8:315
13. Liao H, Chen W, Dai Y et al (2019) Expression of programmed cell death-ligands in hepatocellular carcinoma: correlation with immune microenvironment and survival outcomes. Front Oncol 9:883
14. Jin R, Liu C, Zheng S et al (2020) Molecular heterogeneity of anti-PD-1/PD-L1 immunotherapy efficacy is correlated with tumor immune microenvironment in East Asian patients with non-small cell lung cancer. Cancer Biol Med 17:768–781
15. Kuriyama K, Higuchi T, Yokobori T et al (2020) Uptake of positron emission tomography tracers reflects the tumor immune status in esophageal squamous cell carcinoma. Cancer Sci 11:1969–1978
16. Hirakata T, Fujii T, Kurozumi S et al (2020) FDG uptake reflects breast cancer immunological features: the PD-L1 expression and degree of TILs in primary breast cancer. Breast Cancer Res Treat 181:331–338
17. Kasahara N, Kaira K, Bao P et al (2018) Correlation of tumor-related immunity with 18F-FDG-PET in pulmonary squamous-cell carcinoma. Lung Cancer 119:71–77
18. Kasahara N, Kaira K, Yamaguchi K et al (2019) Fluorodeoxyglucose uptake is associated with low tumor-infiltrating lymphocyte levels in patients with small cell lung cancer. Lung Cancer 134:180–186
19. Kaira K, Shimizu K, Kitahara S et al (2018) 2-Deoxy-2-[fluorine-18] fluoro-d-glucose uptake on positron emission tomography is associated with programmed death ligand-1 expression in patients with pulmonary adenocarcinoma. Eur J Cancer 101:181–190
20. Kaira K, Kuji I, Kagamu H (2021) Value of (18)F-FDG-PET to predict PD-L1 expression and outcomes of PD-1 inhibition therapy in human cancers. Cancer Imaging 21:11
21. Togo M, Yokobori T, Shimizu K et al (2020) Diagnostic value of ^{18}F-FDG-PET to predict the tumour immune status defined by tumoural PD-L1 and $CD8^+$tumour-infiltrating lymphocytes in oral squamous cell carcinoma. Br J Cancer 122:1686–1694

22. Greene S, Robbins Y, Mydlarz WK et al (2020) Inhibition of MDSC trafficking with SX-682, a CXCR1/2 inhibitor, enhances NK-cell immunotherapy in head and neck cancer models. Clin Cancer Res 26:1420–1431
23. Zhong LM, Liu ZG, Zhou X et al (2019) Expansion of PMN-myeloid derived suppressor cells and their clinical relevance in patients with oral squamous cell carcinoma. Oral Oncol 95:157–163
24. Dar AA, Patil RS, Pradhan TN et al (2020) Myeloid-derived suppressor cells impede T cell functionality and promote Th17 differentiation in oral squamous cell carcinoma. Cancer Immunol Immunother 69:1071–1086
25. Mortezaee K (2021) Myeloid-derived suppressor cells in cancer immunotherapy-clinical perspectives. Life Sci 277:119627
26. Ni HH, Zhang L, Huang H et al (2020) Connecting METTL3 and intratumoural CD33(+) MDSCs in predicting clinical outcome in cervical cancer. J Transl Med 18:393
27. Woo JW, Chung YR, Kim M et al (2021) Prognostic significance of S100A8-positive immune cells in relation to other immune cell infiltration in pre-invasive and invasive breast cancers. Cancer Immunol Immunother 70:1365–1378
28. Li Z, Wang J, Zhang X, Liu P et al (2020) Proinflammatory S100A8 induces PD-L1 expression in macrophages, mediat tumor immune escape. J Immunol 204:2589–2599
29. Kim JW, Dang CV (2006) Cancer's molecular sweet tooth and the Warburg effect. Cancer Res 66:8927–8930
30. Hasegawa O, Satomi T, Kono M et al (2019) Correlation between the malignancy and prognosis of oral squamous cell carcinoma in the maximum standardized uptake value. Odontology 107:237–243
31. Minn H, Joensuu H, Ahonen A et al (1998) Fluorodeoxyglucose imaging: a method to assess the proliferative activity of human cancer in vivo. Comparison with DNA flow cytometry in head and neck tumors. Cancer 61:1776–1788
32. Allal AS, Dulguerov P, Allaoua M et al (2002) Standardized uptake value of 2-[(18)F] fluoro-2-deoxy-D-glucose in predicting outcome in head and neck carcinomas treated by radiotherapy with or without chemotherapy. J Clin Oncol 20:1398–1404
33. Suzuki H, Fukuyama R, Hasegawa Y et al (2009) Tumor thickness, depth of invasion, and Bcl-2 expression are correlated with FDG-uptake in oral squamous cell carcinomas. Oral Oncol 45:891–897
34. Zheng D, Niu L, Liu W et al (2019) Correlation analysis between the SUVmax of FDG-PET/CT and clinicopathological characteristics in oral squamous cell carcinoma. Dentomaxillofac Radiol 48:20180416
35. Kaira K, Endo M, Abe M et al (2010) Biologic correlation of 2-[18F]-fluoro-2-deoxy-D-glucose uptake on positron emission tomography in thymic epithelial tumors. J Clin Oncol 28:3746–3753
36. Chang YL, Yang CY, Lin MW et al (2016) High co-expression of PD-L1 and HIF-1α correlates with tumour necrosis in pulmonary pleomorphic carcinoma. Eur J Cancer 60:125–135
37. Ruf M, Moch H, Schraml P (2016) PD-L1 expression is regulated by hypoxia inducible factor in clear renal cell carcinoma. Int J Cancer 139:396–403
38. Noman MZ, Desantis G, Janji B et al (2014) PD-L1 is a novel direct target of HIF-1α, and its blockade under hypoxia enhanced MDSC-mediated T cell activation. J Exp Med 211:781–790
39. Chen R, Zhou X, Liu J et al (2019) Relationship between the expression of PD-1/PD-L1 and ^{18}F-FDG uptake in bladder cancer. Eur J Nucl Med Mol Imaging 46:848–854
40. Chiu DK, Tse AP, Xu IM et al (2017) Hypoxia inducible factor HIF-1 promotes myeloid-derived suppressor cells accumulation through ENTPD2/CD39L1 in hepatocellular carcinoma. Nat Commun 8:517
41. Mabuchi S, Komura N, Sasano T et al (2020) Pretreatment tumor-related leukocytosis misleads positron emission tomography-computed tomography during lymph node staging in gynecological malignancies. Nat Commun 11:1364
42. Lenouvel D, González-Moles MÁ, Ruiz-Ávila I et al (2020) Prognostic and clinicopathological significance of PD-L1 overexpression in oral squamous cell carcinoma: a systematic review and comprehensive meta-analysis. Oral Oncol 106:104722

Publisher's Note